Letter

Spectroscopy along flerovium decay chains. II. Fine structure in odd-A ^{289}Fl

D. M. Cox,[1,*] A. Såmark-Roth,[1] D. Rudolph,[1] L. G. Sarmiento,[1] R. M. Clark,[2] J. L. Egido,[3] P. Golubev,[1] J. Heery,[4,†] A. Yakushev,[5,6] S. Åberg,[1] H. M. Albers,[5] M. Albertsson,[1] M. Block,[5,6,7] H. Brand,[5] T. Calverley,[4] R. Cantemir,[5] B. G. Carlsson,[1] Ch. E. Düllmann,[5,6,7] J. Eberth,[8] C. Fahlander,[1] U. Forsberg,[1] J. M. Gates,[2] F. Giacoppo,[5,6] M. Götz,[5,6,7] S. Götz,[5,6,7] R.-D. Herzberg,[4] Y. Hrabar,[1] E. Jäger,[5] D. Judson,[4] J. Khuyagbaatar,[5,6] B. Kindler,[5] I. Kojouharov,[5] J. V. Kratz,[7] J. Krier,[5] N. Kurz,[5] L. Lens,[5,7,‡] J. Ljungberg,[1] B. Lommel,[5] J. Louko,[9] C.-C. Meyer,[6,7] A. Mistry,[10,5] C. Mokry,[6,7] P. Papadakis,[4,§] E. Parr,[5] J. L. Pore,[2] I. Ragnarsson,[1] J. Runke,[5,7] M. Schädel,[5] H. Schaffner,[5] B. Schausten,[5] D. A. Shaughnessy,[11] P. Thörle-Pospiech,[6,7] N. Trautmann,[7] and J. Uusitalo[9]

[1]*Department of Physics, Lund University, 22100 Lund, Sweden*
[2]*Nuclear Science Division, Lawrence Berkeley National Laboratory, Berkeley, California 94720, USA*
[3]*Departamento de Física Teórica and CIAFF, Universidad Autónoma de Madrid, 28049 Madrid, Spain*
[4]*Department of Physics, University of Liverpool, Liverpool L69 7ZE, United Kingdom*
[5]*GSI Helmholtzzentrum für Schwerionenforschung GmbH, 64291 Darmstadt, Germany*
[6]*Helmholtz Institute Mainz, 55099 Mainz, Germany*
[7]*Department Chemie-Standort TRIGA, Johannes Gutenberg-Universität Mainz, 55099 Mainz, Germany*
[8]*Institut für Kernphysik, Universität zu Köln, 50937 Köln, Germany*
[9]*Department of Physics, University of Jyväskylä, 40014 Jyväskylä, Finland*
[10]*Institut für Kernphysik, Technische Universität Darmstadt, 64289 Darmstadt, Germany*
[11]*Nuclear and Chemical Sciences Division, Lawrence Livermore National Laboratory, Livermore, California 94550, USA*

(Received 12 April 2022; revised 1 September 2022; accepted 16 December 2022; published 6 February 2023)

Fifteen correlated α-decay chains starting from the odd-A superheavy nucleus ^{289}Fl were observed following the fusion-evaporation reaction ^{48}Ca + ^{244}Pu. The results call for at least two parallel α-decay sequences starting from at least two different states of ^{289}Fl. This implies that close-lying levels in nuclei along these chains have quite different spin-parity assignments. Further, observed α-electron and α-photon coincidences, as well as the α-decay fine structure along the decay chains, suggest a change in the ground-state spin assignment between ^{285}Cn and ^{281}Ds. Our experimental results, on the excited level structure of the heaviest odd-N nuclei to date, provide a direct testing ground for theory. This is illustrated by comparison with new nuclear structure calculations based on the symmetry-conserving configuration mixing theory.

DOI: 10.1103/PhysRevC.107.L021301

Alongside the search for new elements ($Z > 118$) [1–6], increasingly sophisticated experimental efforts aim to determine basic chemical properties [7–9], or to collect nuclear structure information on the heaviest elements [10–18]. In this Letter, we report spectroscopic data along 15 α-decay chains originating from ^{289}Fl, including α-electron and α-photon coincidences. The spectroscopic information obtained has allowed us to probe details of the nuclear structure of these nuclei for the first time.

Prior to this work, five decay chains were assigned to ^{289}Fl in the course of the discovery of element 114, based on data obtained at the Dubna Gas-Filled Recoil Separator (DGFRS) [19–21]. Correlated ^{289}Fl recoil-α-α-fission events were confirmed a few years later in experiments behind the Transactinide Separator and Chemistry Apparatus (TASCA) at the GSI Helmholtzzentrum für Schwerionenforschung in Darmstadt, Germany (eight chains, including one reaching ^{277}Hs) [9,22–24]. In several element-116 experiments, ^{289}Fl was observed nine times as α-decay daughter of ^{293}Lv [25–29]. The aggregated decay-energy spectra, correlation times, as well as a statistical assessment, are summarised in Figs. 1 and 2 [panels (a)–(i)] and Table II in the Supplemental Material [30]. Rather broad α-decay energy distributions emerge around $E_\alpha \approx 9.80$ for ^{289}Fl and 9.15 MeV for ^{285}Cn. This hints at a fine structure. However, the correlation-time analysis is consistent with one central decay path and yields rather long half-lives of $T_{1/2} \approx 2$, ≈30, and ≈15 s for ^{289}Fl, ^{285}Cn, and ^{281}Ds, respectively.

*Corresponding author: danielcox404@gmail.com
†Present address: Department of Physics, University of Surrey, Guildford GU2 7XH, United Kingdom.
‡Present address: Institut für Physikalische Chemie und Radiochemie, Hochschule Mannheim, 68163 Mannheim, Germany.
§Present address: STFC Daresbury Laboratory, Daresbury, Warrington WA4 4AD, United Kingdom.

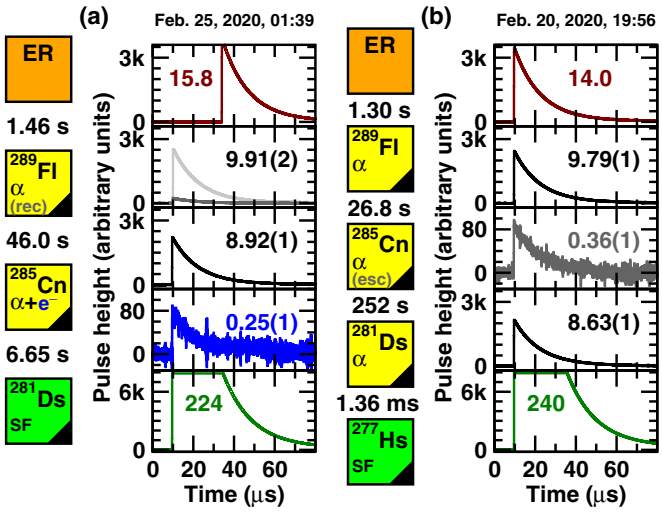

FIG. 1. Digitized preamplifier pulses of events associated with decay chains 27 (a) and 28 (b). Numbers in the panels are calibrated energies in MeV. Correlation times are given between recoil implantation (ER, orange squares), α decays (yellow squares), and fission (green squares). The 9.91(2)-MeV α event in (a) is reconstructed (rec) from pulses in the implantation DSSD [dark grey, 0.95(1) MeV] and an upstream DSSD [grey, 8.15(1) MeV] [16]. The 0.25(1)-MeV event in an upstream DSSD (blue) is in prompt coincidence with the 8.92(1)-MeV event in the implantation DSSD. The 0.36(1)-MeV event in (b) is an α particle escaping (esc) from the implantation DSSD with missed detection in any upstream DSSD. Black triangles in the lower right corner of a square indicate detection during beam-off periods.

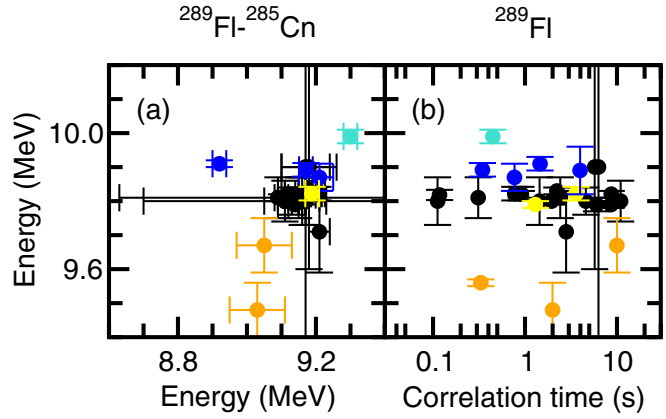

FIG. 2. (a) Energy-energy correlations between α-decay events of ^{289}Fl and ^{285}Cn. (b) Energy-time correlations for ^{289}Fl events. Previous and current data is included. Black circles mark events associated with the main (M) decay branch of ^{289}Fl. Orange and blue circles mark events with low-energy (L) and high-energy (H) α-decay events, respectively, assigned to ^{289}Fl. Yellow circles mark events from the three decay chains ending in ^{277}Hs. Data points in cyan mark chain 17. See decay sequences in Fig. 3 and [30] for more details.

Following a presentation of the key features of the experiment, the identification of the ^{289}Fl decay chains is described. Spectroscopic information is used in conjunction with energy-energy, energy-time, and time-time correlations along the ^{289}Fl decay chains to suggest a decay scheme of ^{289}Fl. A self-consistency check of the proposed decay scheme is performed with GEANT4 simulations. The proposed decay schemes are then compared with the symmetry-conserving configuration mixing theory.

The experiment has been described in detail in Refs. [15,16,31]. In brief, in a two-part experiment conducted at GSI Darmstadt, the fusion-evaporation reactions ^{48}Ca + ^{242,244}Pu were used to collect spectroscopic information on flerovium isotopes. The Universal Linear Accelerator (UNILAC) focused $\gtrsim 4 \times 10^{12}$ ^{48}Ca^{10+} ions per s (time averaged) onto the target wheel [32] in front of TASCA [33,34]. For the targets, Pu was electroplated onto 2.2–2.3 μm thin Ti foils [35]. Target segments were attached to the target wheel such that the backing foils faced the beam. The wheel rotated synchronously with the UNILAC's pulsed beam structure [32], i.e., 5 ms beam on and 15 ms beam off. In the first part of the experiment, one out of four target segments comprised enriched ^{242}Pu with an effective thickness of 0.71(1) mg/cm^2. The other three segments and all four segments in the second part of the experiment were made of ^{244}Pu, with an average thickness of 0.80(1) mg/cm^2 [16]. A bombarding energy of 6.02 MeV/nucleon was used. In combination with 5.0–5.1 μm and 5.5–5.6 μm Ti degrader foils, beam energies of ≈241 and 237 MeV [36], respectively, resulted at the beginning of the Pu target layers [16].

TASCA was filled with 0.8 mbar He gas [37]. The magnetic rigidity of the TASCA dipole magnet was set to $B\rho$ = 2.27 Tm [9,23,24]. With these settings, TASCA transmitted, selected, and focused [38,39] fusion-evaporation products into an upgraded version [15,31] of TASISpec [40]. Its open box configuration of five double-sided silicon strip detectors (DSSD) was complemented with a sixth 'veto' DSSD placed behind the downstream implantation DSSD [15,31]. In addition, a novel Compex-detector module, comprising four encapsulated, cubic-shaped high-purity Ge crystals [41], was positioned behind each of the upstream box DSSDs. A former EUROBALL Cluster detector [42] remained behind the implantation-veto layer. Finally, the read-out electronics were fully digital, and a revised beam-shutoff routine was used. Here, an implantation-like event followed by a promising α-decay candidate event caused an electrostatic chopper to cut the beam pulses in <20 μs. This allowed for low-background measurements of subsequent decays for typical periods of 200–300 s [16,17].

For the even-odd isotope ^{289}Fl, a search for time- and position-correlated recoil-α-α(-α)-fission sequences was conducted using criteria detailed in [16]. A decision tree yielded a probability of 86(3)% to identify ^{289}Fl decay chains compliant with the search criteria [16,17]. The 15 decay chains associated with ^{289}Fl are in detail presented in Table I in the Supplemental Material. The decay-energy spectra and correlation times, also combined with previous data, are shown in Figs. 1(j)–1(o) and 2(j)–2(o) and summarized in the rightmost columns of Table II in the Supplemental Material [30]. Only three α-decay steps were accompanied by prompt photons (two such steps were in decay chain 16 and one in chain 26,

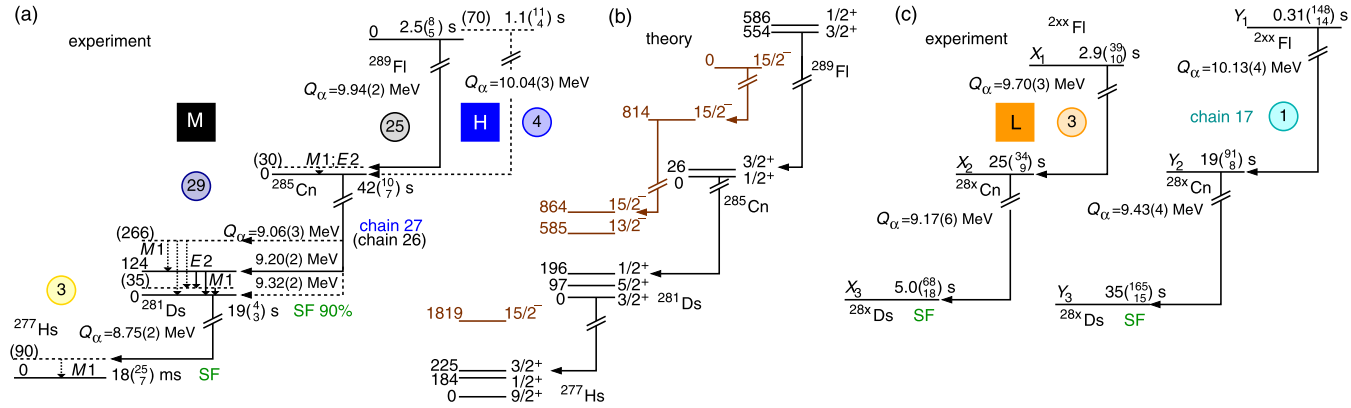

FIG. 3. (a) Proposed main (M + H) experimental and (b) calculated α-decay scheme of ^{289}Fl ($\pi = +$ black, $\pi = -$ brown). Additional decay branches starting with either a low-energy (L) α event or chain 17 are shown in (c). For (a) and (c), numbers in colored circles denote the total number of chains assigned to the respective branch. Half-life values are provided for states decaying by α decay or spontaneous fission (SF). For (a), numbers above the levels are the energies in keV employed in the GEANT4 simulations (cf. Fig. 4). Electromagnetic multipoles, $M1$ or $E2$, correspond to those used in the GEANT4 simulations. For (a), dashed lines and level energies in parentheses indicate tentative levels and decays owing limited statistics.

see Table I in [30]). Statistically, one of them is expected to be of random origin [16]. For the improved TASISpec set-up with the four Compex detectors [41], the photon detection efficiency approaches 50% in the energy range of prime interest (120–150 keV) [18,40]. Furthermore, two prompt ($\Delta t <$ 50 ns) α-electron coincidences were detected, one each in chains 26 and 27. Once above the energy threshold, $E_{\text{thresh}} \approx$ 100 keV, the detection efficiency for electrons in the upstream box DSSDs is purely geometric at 30% [40]. As an example, details of the decay sequence of chain 27 are presented in Fig. 1(a). It shows the detector signals associated with the various decay steps of the event.

As described above, electromagnetic decays (either photons, conversion electrons, or both) were seen in coincidence with only four α-decay steps out of a total of 32 α-decay steps across all 15 observed decay chains. However, these observations are already sufficient to definitively indicate the presence of low-lying excited states in these superheavy nuclei and allow us to build possible decay scenarios as discussed below.

Two of the 15 chains were found to be compatible with the previously observed single decay chain terminating with the suggested fission of ^{277}Hs [22,23]. The half-life was determined to be $T_{1/2,\text{SF}}(^{277}\text{Hs}) = 18(^{25}_{7})$ ms based on all three events [30]. The implantation and decay series of one of these chains is illustrated in Fig. 1(b).

Correlation times from all previous and present studies along decay chains involving ^{289}Fl were combined and analysed according to Refs. [43,44] (cf. Table II in [30]). Energy-energy correlations for ^{289}Fl - ^{285}Cn are plotted in Fig. 2(a). Clearly, the majority of chains accumulate around $E_\alpha(^{289}\text{Fl}) \approx 9.80$ and $E_\alpha(^{285}\text{Cn}) \approx 9.15$ MeV. These form the main (M, black circles) decay branch, the proposed decay scheme of which is focused upon in Fig. 3(a). Data points marked yellow in Fig. 2 correspond to the three chains ending in Hs. Neither in Fig. 2 nor in any other correlation [30] do they exhibit any statistical inconsistency. Therefore, they are considered to be part of the main branch. Two low-energy (L, orange circles) events can be discriminated in Fig. 2(a). They were populated via ^{293}Lv decays in previous data [27,29]. A third event, stemming from chain 22 in our data, is included in Fig. 2(b), which presents energy-time correlations of the first ^{289}Fl decay step. These events could start from the same state (presumably the ground state) in ^{289}Fl as the main branch: Their $T_{1/2}(^{289}\text{Fl}) = 2.9(^{39}_{10})$ s is fully compatible with the $T_{1/2}(^{289}\text{Fl}) = 2.5(^{8}_{5})$ s of the main branch (M) [30]. However, assuming the same starting level for the M and L branches, these L chains would end in an excited state with unreasonably high $E_x \approx 0.5$ MeV in ^{281}Ds. Therefore, the combined information on these three chains is displayed separately in Fig. 3(c).

One observed chain (chain 17 shown with the cyan color) was found to be distinctly different from all the other decay chains associated with ^{289}Fl. It is in shown Fig. 3(c) for completeness. It has significantly higher decay energies for both decay steps, 9.99(2) > 9.80 and 9.30(2) > 9.15, see Fig. 2. Therefore, it cannot be incorporated in the main decay sequence of ^{289}Fl, while an assignment to ^{290}Fl is unfavored based on the half-life of the terminating fission [16].

It is possible to distinguish four additional high-energy (H, blue circles) events in Fig. 2. These are proposed to merge with the main decay branch in the ground state of ^{285}Cn, starting from a second α-decaying state of ^{289}Fl at some 70-keV excitation energy, $T_{1/2} = 1.1(^{11}_{4})$ s, and hindrance factor, HF $\approx$ 2–3 [30,45]. For the remaining decay steps, however, there is no evidence that these four decay chains should be assigned as anything other than members of the main branch.

We now turn to comparing our results to calculations. There are predictions in the available literature of the one quasineutron states in the relevant nuclei [46,47]. However, our observations of low-lying excited level structure in ^{289}Fl and ^{285}Cn immediately suggest that these calculations will not yield even a qualitative agreement with experiment. For instance, Ćwiok *et al.* [46] do not find a single excited state below 0.5 MeV in either ^{289}Fl or ^{285}Cn, in contradiction with the data. Therefore, we turn to a new set of calculations based on the symmetry conserving configuration mixing (SCCM)

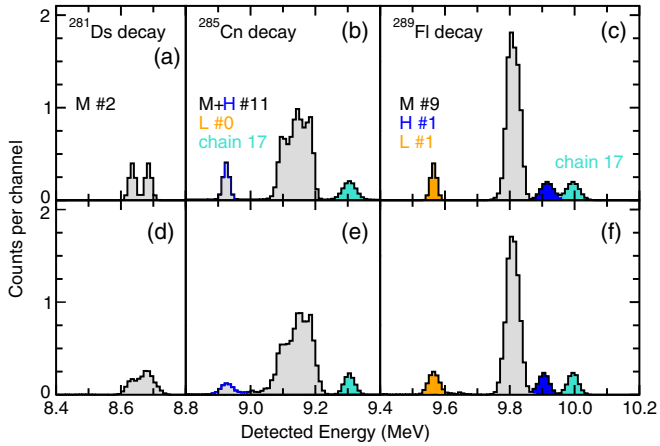

FIG. 4. Comparison of total measured [(a)–(c), experimental data points are represented with a Gaussian of integral one and a width compliant with its measured systematical uncertainty, see [30] for more details] and simulated (d)–(f) decay-energy spectra for ^{289}Fl (c),(f), ^{285}Cn (b),(e), and ^{281}Ds (a),(d). The GEANT4 simulations take the proposed ^{289}Fl decay scheme of Fig. 3 as physics input. The blue lines in (b) and (e) indicates the events feeding from the high-energy into the main branch. The simulated spectra are normalised to the number of observed events per main (M), low-energy (L, orange), or high-energy (H, blue) branch. See text for details.

theory [48–50]. The SCCM approach uses the finite-range density-dependent Gogny force in its D1S parametrization [51] and probes nuclear deformations in the (β, γ) plane. The calculations are similar to those in Refs. [15,52,53], where even-even superheavy nuclei are described. They are state of the art and consider linear combinations of product wave functions (previously projected to the appropriate quantum numbers) obtained by taking the nuclear deformations (β, γ) as generator coordinates in terms of the generator coordinate method. A configuration space of 13 harmonic oscillator major shells has been considered. A convergence test with 17 shells was performed for the ground state of even-even superheavy nuclei. See Ref. [52] for further technical details of the calculations.

In the theoretical calculations shown in Fig. 3(b), we find coexisting positive and negative-parity states. Whereas in ^{285}Cn, ^{281}Ds, and ^{277}Hs the lowest negative-parity states are predicted above the positive-parity ones, in ^{289}Fl it is the opposite. This is probably due to the sharp shape phase transition observed in this region (see Fig. 1 of Ref. [53]). The calculations predict very low-lying excited states in very good qualitative agreement with the experimental observations. This is outlined in the following.

In the present experiment, 12 of the 15 decay chains associated with ^{289}Fl have complete spectroscopic information, i.e., no decay steps escaped detection. Figure 4(a)–4(c) shows the decay-energy spectra of the three α-decaying steps. Each individual data point is represented as a Gaussian of integral one and width compliant to its measured systematic uncertainty. The experimental spectra were interrogated with GEANT4 simulations. The results, based on the physics input of the decay schemes suggested in Fig. 3, are provided in Fig. 4(d)–4(f). The simulations follow the principles outlined in Refs. [54,55], which include Auger-electron and x-ray emission as part of the atomic relaxation process.

Looking at the ^{285}Cn $\rightarrow$ ^{281}Ds decay step, there is the clear triple-peak structure seen in Fig. 4(b) around 9.15 MeV, which indicates α-decay fine structure, consistent with the observed α-photon and α-e^- coincidence events. For this main branch, there is no statistical indication that the decay of ^{281}Ds proceeds from more than one state [30]. A triplet structure is most easily understood by main α-decay feeding into an excited state with $E_x < B_e(K) = 182$ keV [56], which reaches the ground state either directly or by cascading down via an intermediate state by electromagnetic transitions, i.e., conversion electrons or possibly γ rays [57]. Based on the overall width of the triplet in Fig. 4(b), the energy difference between these two low-lying excited states must be around 80–100 keV. The α-decay energies measured for chains 15 and 25, $E_\alpha = 9.18(1)$ MeV, and the 8.92(1)-0.25(1)-MeV α-electron event [chain 27, see Fig. 1(a)] are used to restrict $Q_\alpha \approx 9.31$ MeV. The latter requires another excited state in ^{281}Ds at $E_x \gtrsim 0.27$ MeV, as B_e(L,Ds) = 26–37 keV [56].

The clear observation of such an α-decay fine structure pattern is important. It immediately shows that the isotopic assignment of the decay chains to an odd-A nucleus is correct, since an even-even nucleus is unlikely to display such a complex decay pattern. Moreover, the observation of electromagnetic decays linking a sequence of states at low-excitation energy to the ground state restricts predictions of the level structure. These sequences are unlikely to involve a low-lying unique-parity high-j intruder because the electromagnetic decay of such a state would be strongly disfavored. Moreover, α decay is generally favored between states of the same spin and parity. To observe a sequence of electromagnetic transitions following the ground state α decay of ^{285}Cn therefore implies that the ground-state spin of the daughter nucleus, ^{281}Ds, is different to that of the parent, ^{285}Cn. One sees that even the limited information on excited states can already provide stringent tests of model calculations.

Figure 3(a) displays one possible scenario. Here, the excitation energy of the state at $E_x = 0.124$ MeV is suggested by an α-photon coincidence (chain 16). In combination with $Q_\alpha = 9.20(2)$ MeV, an intermediate state at $\approx$35 keV, a 70 : 30 branching ratio for the anticipated electromagnetic transitions, and an $\approx$20% α branch into the ground state [$Q_\alpha = 9.32(2)$ MeV], the GEANT4 simulation displayed in Fig. 4(e) becomes consistent with experiment seen in Fig. 4(b). In this scenario, the 0.25(1)-MeV electron in chain 27 is stemming from an $E2$ transition ($\alpha_{\rm tot} \approx 1.1$, $\alpha_{\rm L} \approx 0.7$, $\alpha_{\rm M} \approx 0.2$ [58]) from the tentative state at $E_x = 266$ keV, in view of the 142-keV photon detected in chain 26. With $Q_\alpha = 9.06(3)$ MeV, the 8.92-MeV α event appears at a consistent position in the simulation. Within 2σ, the 0.14(1)-MeV electron observed in chain 26 matches an M or higher-shell conversion electron from the 124-keV level. Unfortunately, that chain lacks full α-decay energy information for this decay step, which renders its information content much less valuable.

Continuing with the ^{281}Ds $\rightarrow$ ^{277}Hs decay step, two α-decay events are at hand. They have decay energies measured at 8.63(1) and 8.68(1) MeV. Figure 4(d) shows that a

consistent description of these events can be readily achieved by interpreting the higher-energy event as sum of an 8.63-MeV α particle (HF $\approx$ 1 [30]) with an $\approx$60-keV L-conversion electron. This originates from an $\approx$90-keV $M1$ or $E2$ transition with $\alpha_{\mathrm{tot}} \approx 35$ and 90, respectively [58]. It is worth noting that the third data point, namely an α-decay event with 8.71(2) MeV measured in a previous TASCA experiment [22,23], is consistent. The suggested decay pattern in Fig. 3(a), including the low hindrance factor, is in good agreement with the calculations, which predict a decay from a $3/2^+$ ground state of ^{281}Ds into an excited $3/2^+$ state in ^{277}Hs, some 40 keV above a $1/2^+$ state, which in turn undergoes fission rather than an $M4$ or $E5$ decay into the predicted $9/2^+$ ground state of ^{277}Hs.

Up to this point, we have not discussed the spectrum observed for the first decay step, $^{289}\mathrm{Fl} \rightarrow {}^{285}\mathrm{Cn}$ which is shown in Fig. 4(c). It comprises four α-decay lines corresponding to chain 17 as well as the main (M), high-energy (H), and low-energy (L) events defined earlier. In the simulations, the decay of the main branch is best described if there is a low-lying state of $\approx$30 keV in ^{285}Cn, which decays with a highly converted $M1$ or $E2$ transition into the ground state of ^{285}Cn. Summing of α- and conversion-electron energies provides an explanation for a likely increase in the width of the peak, measured as 43(9) keV compared with 35(2) keV expected at $E_\alpha = 10$ MeV [17]. The comparison of measured and simulated spectra is seen in Figs. 4(c) and 4(f).

The observed main decay branch (M) in Fig. 3(a) readily finds its explanation in a sequence of predicted (alternating) low-spin positive-parity states. Adjacent is another calculated decay sequence indicated in Fig. 3(b), which is built upon high-j negative-parity states, and which is energetically compressed with respect to the low-spin positive-parity states. In the experiment, the three low-energy (L) events, depicted in Fig. 3(c), could thus be associated with the predicted high-j sequence, though their compression is less pronounced than calculated.

To summarize, an experiment was conducted behind the TASCA separator at GSI Darmstadt, aiming to perform high-resolution decay spectroscopy on flerovium ($Z = 114$). Owing to the unique combination of the pulsed-beam structure provided by the UNILAC, an advanced beam-shutoff routine allowing for low background correlations over several minutes, and the high-resolution decay-spectroscopy setup, fifteen decay chains from ^{289}Fl were registered and found to provide definitive evidence for fine structure for the first time. The ground state, and at least one excited state, in ^{289}Fl α decay to states in the daughter ^{285}Cn. The ^{285}Cn ground state in turn populates multiple states in ^{281}Ds and we have found evidence for electromagnetic decays between those states implying low multipolarity changes ($M1$, $E2$). This suggests a low-lying sequence of natural parity states. The pattern of decay also implies a change in the ground-state spin-parity between ^{285}Cn and ^{281}Ds. A series of lower-energy α transitions along the decay chains may be indicative of a parallel decay pathway. It is suggested that this parallel decay involves unique-parity high-j intruder states which will not have favored decay pathways to the natural parity states. Such basic information from fine structure studies, ours being the first for these superheavy even-Z–odd-N nuclei, already challenges theory. This was demonstrated by comparison with new SCCM, calculations, which have been shown to have consistency with our observations. For instance, the predictions of the main decay branch of ^{289}Fl, including its fine-structure aspects, is found to be consistent with the suggestion of a sequence of low-spin positive-parity states for ^{289}Fl decaying via ^{285}Cn and ^{281}Ds into ^{277}Hs.

The results presented here are based on the experiment U310, which was performed at the beam line X8/TASCA at the GSI Helmholtzzentrum für Schwerionenforschung, Darmstadt (Germany) in the frame of FAIR Phase-0. The authors would like to thank the ion-source and accelerator staff at GSI for their supreme efforts. This work has received funding from the European Union's Horizon 2020 research and innovation programme under Grant Agreement No. 654002 (ENSAR2). The ^{244}Pu target material was provided by the U.S. DOE through ORNL. The Lund group is indebted to decisive support from the Knut and Alice Wallenberg foundation (KAW 2015.0021), and we highly appreciate the possibility to collaborate with the workshops at IKP Köln. This work was also supported by the Swedish Research Council (Vetenskapsrådet, VR 2016-3969), the Royal Physiographic Society in Lund, the Spanish Ministerio de Ciencia e Inovación under Contract No. PID2020-118265GB-C41, the German BMBF (05P18UMFN2), the U.S. DOE under Contract No. DE-AC02-05CH11231 (LBNL), and the UK STFC.

[1] Yu. Ts. Oganessian, V. K. Utyonkov, Yu. V. Lobanov, F. Sh. Abdullin, A. N. Polyakov, R. N. Sagaidak *et al.*, Phys. Rev. C **79**, 024603 (2009).
[2] Yu. Ts. Oganessian and V. K. Utyonkov, Nucl. Phys. A **944**, 62 (2015).
[3] Ch. E. Düllmann, EPJ Web Conf. **131**, 08004 (2016).
[4] S. Hofmann, S. Heinz, R. Mann, J. Maurer, G. Münzenberg, S. Antalic *et al.*, Eur. Phys. J. A **52**, 180 (2016).
[5] F. P. Heßberger and D. Ackermann, Eur. Phys. J. A **53**, 123 (2017).
[6] J. Khuyagbaatar, A. Yakushev, Ch. E. Düllmann, D. Ackermann, L.-L. Andersson, M. Asai *et al.*, Phys. Rev. C **102**, 064602 (2020).
[7] A. Türler, R. Eichler, and A. Yakushev, Nucl. Phys. A **944**, 640 (2015).
[8] A. Yakushev and R. Eichler, EPJ Web Conf. **131**, 07003 (2016).
[9] A. Yakushev, L. Lens, Ch. E. Düllmann, J. Khuyagbaatar, E. Jäger, J. Krier *et al.*, Front. Chem. **10**, 976635 (2022).
[10] D. Ackermann, Nucl. Phys. A **944**, 376 (2015).
[11] D. Rudolph, U. Forsberg, P. Golubev, L. G. Sarmiento, A. Yakushev, L.-L. Andersson *et al.*, Phys. Rev. Lett. **111**, 112502 (2013).
[12] J. M. Gates, K. E. Gregorich, O. R. Gothe, E. C. Uribe, G. K. Pang, D. L. Bleuel *et al.*, Phys. Rev. C **92**, 021301(R) (2015).
[13] U. Forsberg, D. Rudolph, L.-L. Andersson, A. Di Nitto, Ch. E. Düllmann, C. Fahlander *et al.*, Nucl. Phys. A **953**, 117 (2016).

[14] Y. Shi, D. E. Ward, B. G. Carlsson, J. Dobaczewski, W. Nazarewicz, I. Ragnarsson, and D. Rudolph, Phys. Rev. C **90**, 014308 (2014).

[15] A. Såmark-Roth, D. M. Cox, D. Rudolph, L. G. Sarmiento, B. G. Carlsson, J. L. Egido *et al.*, Phys. Rev. Lett. **126**, 032503 (2021).

[16] A. Såmark-Roth, D. M. Cox, D. Rudolph, L. G. Sarmiento, M. Albertsson, B. G. Carlsson *et al.*, Phys. Rev. C **107**, 024301 (2023).

[17] A. Såmark-Roth, Spectroscopy along decay chains of element 114, flerovium, Ph.D. thesis, Lund University, 2021.

[18] D. Rudolph, Eur. Phys. J. A **58**, 242 (2022).

[19] Yu. Ts. Oganessian, V. K. Utyonkov, Yu. V. Lobanov, F. Sh. Abdullin, A. N. Polyakov, I. V. Shirokovsky *et al.*, Phys. Rev. C **62**, 041604(R) (2000).

[20] Yu. Ts. Oganessian, V. K. Utyonkov, Yu. V. Lobanov, F. Sh. Abdullin, A. N. Polyakov, I. V. Shirokovsky *et al.*, Phys. Rev. C **69**, 054607 (2004).

[21] Yu. Oganessian, J. Phys. G **34**, R165 (2007).

[22] Ch. E. Düllmann, M. Schädel, A. Yakushev, A. Türler, K. Eberhardt, J. V. Kratz *et al.*, Phys. Rev. Lett. **104**, 252701 (2010).

[23] J. M. Gates, Ch. E. Düllmann, M. Schädel, A. Yakushev, A. Türler, K. Eberhardt *et al.*, Phys. Rev. C **83**, 054618 (2011).

[24] A. Yakushev, J. M. Gates, A. Türler, M. Schädel, Ch. E. Düllmann, D. Ackermann *et al.*, Inorg. Chem. **53**, 1624 (2014).

[25] Yu. Ts. Oganessian, V. K. Utyonkov, Yu. V. Lobanov, F. Sh. Abdullin, A. N. Polyakov, I. V. Shirokovsky *et al.*, Phys. Rev. C **63**, 011301(R) (2000).

[26] Yu. Ts. Oganessian, V. K. Utyonkov, and K. J. Moody, Phys. At. Nucl. **64**, 1349 (2001).

[27] Yu. Ts. Oganessian, V. K. Utyonkov, Yu. V. Lobanov, F. Sh. Abdullin, A. N. Polyakov, I. V. Shirokovsky *et al.*, JINR preprint No. E7-2004-160, pp. 1–28 (2004), http://www.jinr.ru/publish/Preprints/2004/160(E7-2004-160).pdf.

[28] S. Hofmann *et al.*, Eur. Phys. J. A **48**, 62 (2012).

[29] D. Kaji, K. Morita, K. Morimoto, H. Haba, M. Asai, K. Fujita *et al.*, J. Phys. Soc. Jpn. **86**, 034201 (2017).

[30] See Supplemental Material at http://link.aps.org/supplemental/10.1103/PhysRevC.107.L021301 for detailed results and statistical assessments concerning decay chains starting with the isotope ^{289}Fl.

[31] D. M. Cox, A. Såmark-Roth, D. Rudolph, L. G. Sarmiento, C. Fahlander, U. Forsberg *et al.*, J. Phys.: Conf. Ser. **1643**, 012125 (2020).

[32] E. Jäger, H. Brand, Ch. E. Düllmann, J. Khuyagbaatar, J. Krier, M. Schädel, T. Torres, and A. Yakushev, J. Radioanal. Nucl. Chem. **299**, 1073 (2014).

[33] A. Semchenkov, W. Brüchle, E. Jäger, E. Schimpf, M. Schädel, C. Mühle *et al.*, Nucl. Instrum. Methods Phys. Res. B **266**, 4153 (2008).

[34] M. Schädel, Eur. Phys. J. D **45**, 67 (2007).

[35] J. Runke, Ch. E. Düllmann, K. Eberhardt, P. A. Ellison, K. E. Gregorich, S. Hofmann *et al.*, J. Radioanal. Nucl. Chem. **299**, 1081 (2014).

[36] J. F. Ziegler, Nucl. Instrum. Methods Phys. Res. B **219-220**, 1027 (2004).

[37] J. Khuyagbaatar, D. Ackermann, L.-L. Andersson, J. Ballof, W. Brüchle, Ch. E. Düllmann *et al.*, Nucl. Instrum. Methods Phys. Res. A **689**, 40 (2012).

[38] K. E. Gregorich, Nucl. Instrum. Methods Phys. Res. A **711**, 47 (2013).

[39] U. Forsberg, Element 115, Ph.D. thesis, Lund University, 2016.

[40] L.-L. Andersson, D. Rudolph, P. Golubev, R.-D. Herzberg, R. Hoischen, E. Merchán *et al.*, Nucl. Instrum. Methods Phys. Res. A **622**, 164 (2010).

[41] A. Såmark-Roth, D. M. Cox, J. Eberth, P. Golubev, D. Rudolph, L. G. Sarmiento, G. Tocabens, M. Ginsz, B. Pirard, and P. Quirin, Eur. Phys. J. A **56**, 141 (2020).

[42] J. Eberth *et al.*, Nucl. Instrum. Methods Phys. Res. A **369**, 135 (1996).

[43] K.-H. Schmidt, C.-C. Sahm, K. Pielenz, and H.-G. Clerc, Z. Phys. A **316**, 19 (1984).

[44] K. H. Schmidt, Eur. Phys. J. A **8**, 141 (2000).

[45] C. Qi, F. R. Xu, R. J. Liotta, R. Wyss, M. Y. Zhang, C. Asawatangtrakuldee, and D. Hu, Phys. Rev. C **80**, 044326 (2009).

[46] S. Ćwiok, W. Nazarewicz, and P. H. Heenen, Phys. Rev. Lett. **83**, 1108 (1999).

[47] A. N. Kuzmina, G. G. Adamian, and N. V. Antonenko, Phys. Rev. C **85**, 027308 (2012).

[48] T. R. Rodríguez and J. L. Egido, Phys. Rev. C **81**, 064323 (2010).

[49] J. L. Egido, Phys. Scr. **91**, 073003 (2016).

[50] M. Borrajo and J. L. Egido, Phys. Rev. C **98**, 044317 (2018).

[51] J. F. Berger, M. Girod, and D. Gogny, Nucl. Phys. A **428**, 23 (1984).

[52] J. L. Egido and A. Jungclaus, Phys. Rev. Lett. **125**, 192504 (2020).

[53] J. L. Egido and A. Jungclaus, Phys. Rev. Lett. **126**, 192501 (2021).

[54] L. G. Sarmiento, L.-L. Andersson, and D. Rudolph, Nucl. Instrum. Methods Phys. Res. A **667**, 26 (2012).

[55] L. G. Sarmiento, EPJ Web Conf. **131**, 05004 (2016).

[56] T. A. Carlson and C. W. Nestor, Jr., At. Data Nucl. Data Tables **19**, 153 (1977).

[57] D. Rudolph, L. G. Sarmiento, and U. Forsberg, AIP Conf. Proc. **1681**, 030015 (2015).

[58] T. Kibédi, T. W. Burrows, M. B. Trzhaskovskaya, P. M. Davidson, and C. W. Nestor, Jr., Nucl. Instrum. Methods Phys. Res. A **589**, 202 (2008).